

Is the Radial Profile of the Phase-Space Density of Dark Matter Haloes a Power-Law?

Chung-Pei Ma^{1*}, Philip Chang¹, and Jun Zhang¹

¹*Department of Astronomy and Theoretical Astrophysics Center, 601 Campbell Hall, University of California, Berkeley, CA 94720*

19 January 2018

ABSTRACT

The latest cosmological N -body simulations find two intriguing properties for dark matter haloes: (1) their radial density profile, ρ , is better fit by a form that flattens to a constant at the halo center (the Einasto profile) than the widely-used NFW form; (2) the radial profile of the pseudo-phase-space density, ρ/σ_r^3 , on the other hand, continues to be well fit by a power law, as seen in earlier lower-resolution simulations. In this paper we use the Jeans equation to argue that (1) and (2) cannot both be true at all radii. We examine the *implied* radial dependence of ρ/σ_r^3 over 12 orders of magnitude in radius by solving the Jeans equation for a broad range of input ρ and velocity anisotropy β . Independent of β , we find that ρ/σ_r^3 is approximately a power law *only* over the limited range of halo radius resolvable by current simulations (down to $\sim 0.1\%$ of the virial radius), and ρ/σ_r^3 deviates significantly from a power-law below this scale for both the Einasto and NFW ρ . The same conclusion also applies to a more general density-velocity relation ρ/σ_D^ϵ . Conversely, when we enforce $\rho/\sigma_r^3 \propto r^{-\eta}$ as an input, none of the physically allowed ρ (occurring for the narrow range $1.8 \lesssim \eta \leq 1.9444$) follows the Einasto form. We expect the next-generation simulations with better spatial resolution to settle the debate: either the Einasto profile will continue to hold and ρ/σ_r^3 will deviate from a power law, or ρ/σ_r^3 will continue as a power law and ρ will deviate from its current parameterizations.

1 INTRODUCTION

N -body simulations of cosmological structure formation have shown that the spherically-averaged radial profiles of the mass density and velocity dispersion of dark matter haloes follow simple and nearly universal functional forms that are largely independent of halo properties such as mass, environment, and formation history. For the density profile ρ , there had been considerable discussion about the value of the logarithmic slope of its central cusp, $\gamma \equiv d \log \rho / d \log r$, whether it is -1 as in the forms of, e.g., Hernquist (1990); Navarro et al. (1997), or -1.5 as in Moore et al. (1999). Results from recent N -body simulations now suggest a lack of a definite inner slope – the density profile of these better-resolved dark matter haloes continues to flatten with shrinking radius (e.g., Navarro et al. 2004; Merritt et al. 2005, 2006; Graham et al. 2006; Navarro et al. 2008; Stadel et al. 2008). Functional forms such as Einasto (1969) and Prugniel & Simien (1997) motivated by the Sersic profile for the surface brightness of galaxies (Sersic 1968) appear to provide a more accurate fit to the latest simulations. In these forms, γ itself is a function of radius and asymptotes to zero at the halo center.

A second property that has attracted much attention lately is the radial profile of the pseudo-phase-space density, ρ/σ^3 , which has been reported to be well approximated by a power-law in a number of N -body simulations (e.g., Taylor & Navarro 2001; Ascasibar et al. 2004; Dehnen &

McLaughlin 2005; Hoffman et al. 2007; Stadel et al. 2008; Navarro et al. 2008). Both the total velocity dispersion and the velocity dispersion in the radial direction have been used to define σ . Unlike the controversial density profile, whose best-fit form has changed over the years with improved numerical resolution, the power-law profile of ρ/σ^3 has withstood the scrutiny, and different studies have all reported similar findings except for a minor variation in the actual value of the slope of the power law.

A third relation was proposed when the velocity anisotropy, $\beta(r) = 1 - \sigma_t^2/\sigma_r^2$, of simulated haloes was taken into account. Hansen & Moore (2006) advocated a linear relation between β and the local logarithmic slope of ρ . Other studies, however, have found a large scatter in this relation, particularly in the outer parts of the haloes beyond the scale radius (Dehnen & McLaughlin 2005; Navarro et al. 2008).

To help elucidate the physical meanings of these empirical relations determined from simulated haloes, a typical approach is to use the Jeans equation for a spherical, self-gravitating collisionless system in equilibrium to predict the density or velocity structures of dark matter haloes under a certain set of assumptions. Most of the recent studies based on this approach have begun with the assumption of a power-law $\rho/\sigma_r^3(r)$. These papers then explored the density profiles allowed by the Jeans equation with either isotropic velocities (e.g. Taylor & Navarro 2001; Hansen 2004), or an anisotropic velocity profile $\beta(r)$ (e.g., Dehnen & McLaughlin

arXiv:0907.3144v1 [astro-ph.CO] 17 Jul 2009

2005; Hansen Stadel 2006). Alternatively, some authors have chosen to study the radial profile of the velocity anisotropy $\beta(r)$ from the Jeans equation, starting with a power-law ρ/σ_r^3 and some input form for ρ (e.g., Zait et al. 2008).

In this paper, we reexamine this question by taking a complementary approach. In Sec. 2, we do not assume a power-law ρ/σ_r^3 , but instead solve for ρ/σ_r^3 using the Jeans equation with input $\rho(r)$ and $\beta(r)$ that are motivated by simulations. We find that while ρ/σ_r^3 is approximately a power law within the radial range probed by the current N -body simulations, it is not universally a power-law and shows significant deviations below this range. This approach (for isotropic velocities) was also used in Graham et al. (2006). While our results for the $\beta = 0$ case agree with theirs in the range of radii explored in their paper (down to $\sim 0.1\%$ of the virial radius r_{vir}), we explore 7 orders of magnitude below this range and predict non-power-law behavior in ρ/σ_r^3 in the upcoming simulations. As we show in Sec. 3, this conclusion remains unchanged when velocity anisotropy is included in the calculation, and when a more general form of the density-velocity relation, ρ/σ_D^ϵ , is considered. For completeness, Sec. 4 compares the results for the case when ρ/σ_r^3 is restricted to be a power law.

2 RESULT: ρ/σ_r^3 IS NOT A POWER-LAW

For a spherical, self-gravitating collisionless system in equilibrium, its density and velocity structures obey the Jeans equation

$$\frac{1}{\rho} \frac{d(\rho\sigma_r^2)}{dr} + \frac{2\sigma_r^2\beta}{r} = -\frac{d\Phi}{dr}, \quad (1)$$

where ρ is the radial density profile, $\beta = 1 - \sigma_t^2/\sigma_r^2$ is the velocity anisotropy parameter, σ_r and σ_t are the one-dimensional radial and tangential velocity dispersions, and Φ is the gravitational potential. To apply the Jeans equation, we take as input a form for ρ and solve for σ_r . For the purposes of this paper, we consider two broad types of radial density profiles. The first type is cuspy all the way to the halo center with an inner logarithmic slope γ and an outer slope γ_∞ :

$$\rho(r) = \frac{\rho_0}{(r/r_{-2})^\gamma [1 + r/r_{-2}]^{\gamma_\infty - \gamma}}, \quad (2)$$

where r_{-2} , often referred to as the scale radius, is the radius at which $d \ln \rho / d \ln r = -2$. Examples of special cases of (γ, γ_∞) that have been proposed for dark matter haloes include $(-1, -3)$ by Navarro et al. (1997), $(-1, -4)$ by Hernquist (1990) and Dubinski & Carlberg (1991), and $(-1.5, -3)$ by Moore et al. (1999). We find very similar results from our calculations for $\gamma_\infty = -3$ vs -4 ; we will thus set $\gamma_\infty = -3$ and refer to equation (2) as GNFW below.

The other type of density profile considered in this paper has a non-cuspy inner profile, given by the Einasto profile (Einasto 1969) advocated in several recent studies (e.g., Merritt et al. 2005; Graham et al. 2006; Navarro et al. 2008; Stadel et al. 2008):

$$\ln \frac{\rho(r)}{\rho_{-2}} = \frac{2}{\alpha} [1 - (r/r_{-2})^\alpha]. \quad (3)$$

This profile has the feature that its logarithmic slope is itself

a power-law in r : $d \ln \rho / d \ln r = -2(r/r_{-2})^\alpha$. Unlike equation (2) that has a definite inner slope of γ , this profile continues to flatten towards the halo center. Equation (3) has the same form as the Sersic profile commonly used to fit the two-dimensional projected surface brightness of galaxies (Sersic 1968). The Sersic index n is simply equal to $1/\alpha$.

Starting with either profile in equation (2) or (3), and $\beta = 0$ or some form of $\beta(r)$, we integrate the Jeans equation (1) to obtain $\sigma_r(r)$. The numerical integration is performed from large radius (typically $r = 10^5 r_{-2}$) down to the radius r of interest, using a standard Runge-Kutta integrator (Press et al. 1992). The velocity dispersion is assumed to be zero at the starting large radius. The σ_r from the integration is then combined with the input $\rho(r)$ to obtain $\rho/\sigma_r^3(r)$.

The left two panels of Fig. 1 shows the result ρ/σ_r^3 (upper panel) and its logarithmic slope (lower panel) over 12 orders of magnitude in halo radius for $\beta = 0$ and both types of input density profiles: GNFW with $\gamma = 0.5, 0.75, 1.0$, and 1.5 (dashed curves), and Einasto with $\alpha = 0.12, 0.16$, and 0.18 (solid curves). The range of α is chosen to span the best-fit values of 0.115 to 0.179 for the six simulated galaxy-size haloes in Navarro et al. (2008). The right two panels of Fig. 1 show zoom-in views of the portion of the left figures that is resolvable by current simulations: $0.01 \lesssim r/r_{-2} \lesssim 10$.

Fig. 1 illustrates that ρ/σ_r^3 is not a power-law in r for any of the seven input density profiles. For GNFW haloes, the slopes of ρ/σ_r^3 exhibit oscillations and deviate noticeably from the critical case $\rho/\sigma_r^3 \propto r^{-1.9}$ (indicated by light dotted straight lines), in particular in the extreme cases of inner cusps of $\gamma = 0.5$ (red dashed) and 1.5 (blue dashed). The Einasto haloes also deviate strongly from a power-law at small radius. The zoom-in panels show, however, that the slopes of ρ/σ_r^3 happen to be quite close to -1.9 over the limited range of $r/r_{-2} \sim 0.01$ to 10 that is resolvable by current simulations. This feature is particularly striking for the Einasto profiles, where all three solid curves for ρ/σ_r^3 have a slope within -2.0 and -1.8 from $r/r_{-2} \sim 0.01$ to 10, with the deviations only starting to show up at the smallest radius $r/r_{-2} \sim 0.01$ near the simulation resolution limit. It is therefore not surprising that the power-law behavior of $\rho/\sigma_r^3(r)$ continues to appear to be valid even though the latest simulations find the Einasto form a better fit for $\rho(r)$ than GNFW – Fig. 1 shows the Einasto profiles in fact predict a more power-law $\rho/\sigma_r^3(r)$ for $r/r_{-2} \gtrsim 0.01$.

The important point to note, however, is at the smaller radius of $r/r_{-2} \lesssim 0.01$ in Fig. 1. Here $\rho/\sigma_r^3(r)$ deviates far away from a pure power law with a wide range of slopes that depend on the input ρ . For Einasto haloes, the shape of ρ/σ_r^3 flattens continuously towards the halo center, reaching the asymptotic value of $d \ln \rho / d \ln r = 0$ at $r = 0$ regardless of the parameter α . This is not unexpected of the Einasto profile as the density approaches an asymptotic value in the core. For GNFW, there are two possibilities. For inner slopes of ρ that are steeper (shallower) than the critical $\gamma \approx 0.75$, the power-law slopes of ρ/σ_r^3 are steeper (shallower) than the critical -1.9 . At the critical $\gamma \approx 0.75$, the GNFW halo has $\rho/\sigma_r^3 \approx r^{-1.9}$ at small r , a result consistent with that of Taylor & Navarro (2001), which showed that starting with an exact power-law of $\rho/\sigma_r^3 \propto r^{-1.875}$, the resulting density profile has an inner slope of $d \ln \rho / d \ln r \approx 0.75$. It is worth noting, however, that even the $\gamma = 0.75$ GNFW halo shows

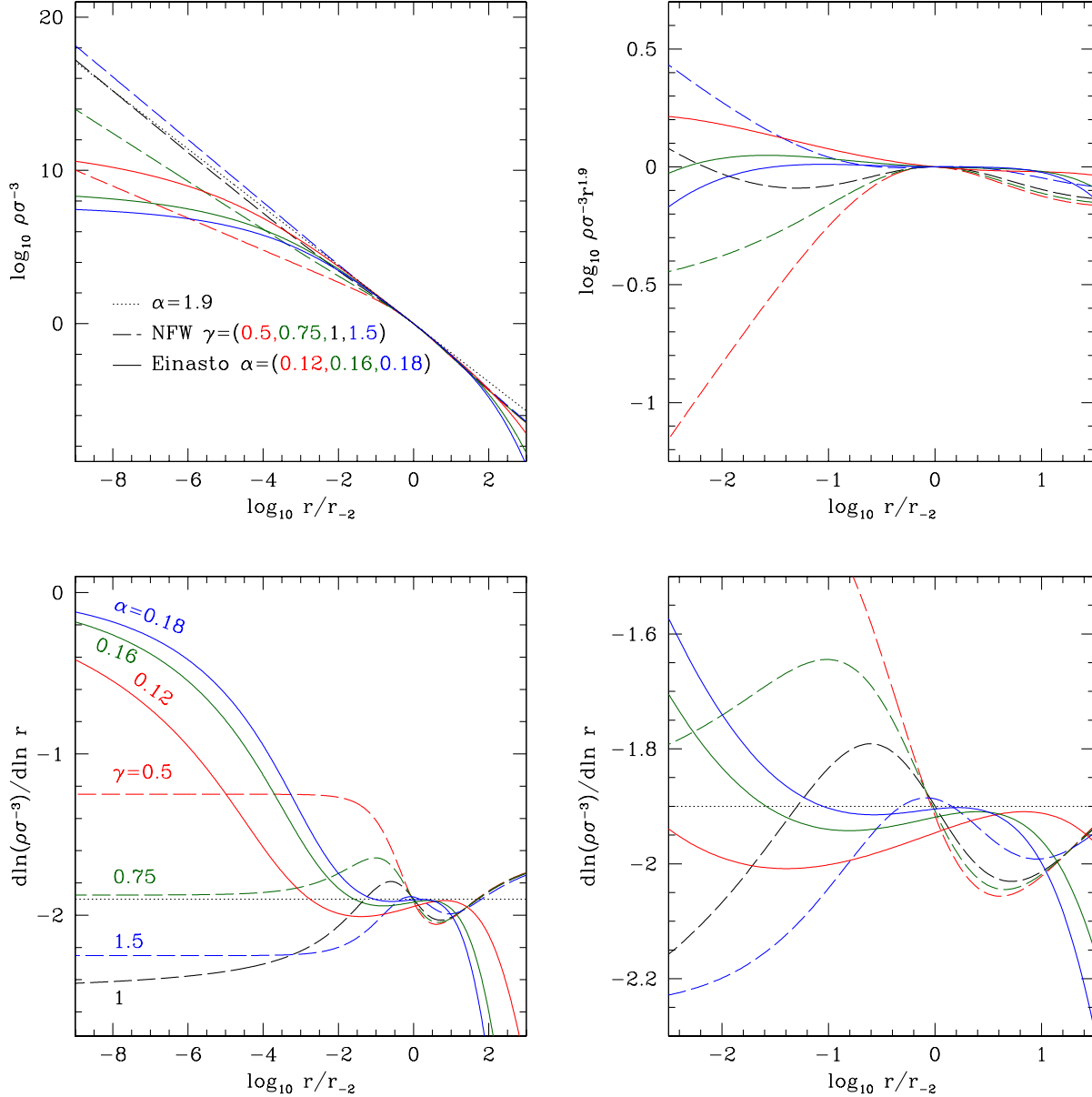


Figure 1. Radial profiles of the pseudo-phase-space density $\rho/\sigma_r^3(r)$ (upper panels) and the corresponding logarithmic slope $d \ln \rho/\sigma_r^3(r)/d \ln r$ (lower panels) obtained from the spherical Jeans equation with $\beta = 0$ for seven input halo density profiles: Einasto (solid) with $\alpha = 0.18$ (blue), 0.16 (green), and 0.12 (red), and GFW (dashed) with $\gamma = 1.5$ (blue), 1 (black), 0.75 (green), and 0.5 (red). The left panels show the behavior of $\rho/\sigma_r^3(r)$ over 12 orders of magnitude in r , while the right panels show zoom-in views of the region $0.01 \lesssim r/r_{-2} \lesssim 10$, which corresponds to the range resolvable by the latest N -body simulations. For ease of comparison with a power-law, the light dotted straight lines indicate the critical case $\rho/\sigma_r^3 \propto r^{-1.9}$, and the y -axis in the upper right panel plots the logarithm of the ratio of $\rho/\sigma_r^3(r)$ to $\rho/\sigma_r^3 \propto r^{-1.9}$. All curves are scaled to have $\rho/\sigma_r^3 = 1$ at $r = r_{-2}$.

wiggles in the corresponding ρ/σ_r^3 profile; that is, no GFW haloes have an exact power-law ρ/σ_r^3 .

3 FURTHER CONSIDERATIONS: ρ/σ_r^3 IS STILL NOT A POWER-LAW

We also find the conclusion reached in Sec. 2 to hold not just for isotropic velocity distributions, but also for anisotropic velocity distributions. To illustrate this point, we solve equa-

tion (1) using an input $\beta(r)$ motivated by N -body simulations (Hansen & Moore 2006; Zait et al. 2008), where β is a function of the local logarithmic slope of the density profile:

$$\beta(r) = -0.2 \left(\frac{d \ln \rho}{d \ln r} + 0.8 \right). \quad (4)$$

We then compute $\rho/\sigma_r^3(r)$ for a similar suite of GFW and Einasto profiles. The results are shown in Fig. 2. What is especially notable is how insensitive the slopes of ρ/σ_r^3 are to the form of $\beta(r)$ used in the calculation. This independence

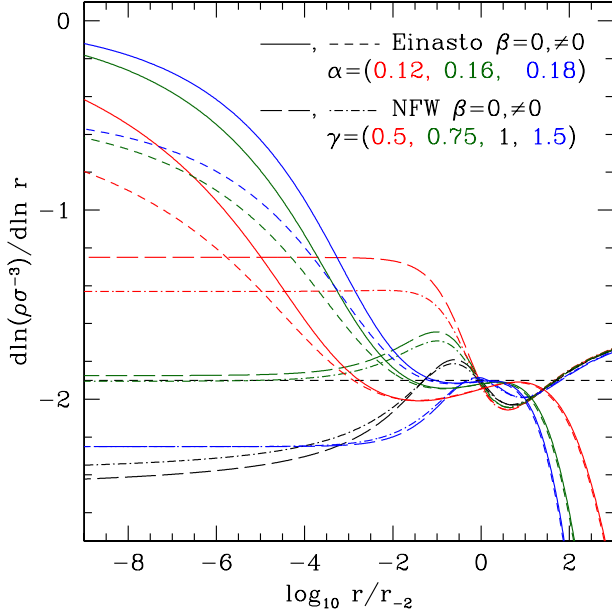


Figure 2. Effects of velocity anisotropy on the radial profile of ρ/σ_r^3 computed from the Jeans equation: $\beta = 0$ (solid for Einasto; long dashed for GNFW; same as lower left panel in Fig. 1), and β given by eq. (4) (short dashed for Einasto; dashed-dotted for GNFW). The seven input density profiles are the same as in Fig. 1. This figure illustrates that including velocity anisotropy in the Jeans equation does not change ρ/σ_r^3 significantly and still results in a non-power-law ρ/σ_r^3 .

from velocity anisotropy strengthens our conclusion reached earlier, namely, that ρ/σ_r^3 is not a power law.

Our findings are also in line with some recent work that has called into question the universality of ρ/σ_r^3 . For instance, Schmidt et al. (2008) has advocated that individual simulated haloes are better fit by a generalized power-law relation that is not necessarily ρ/σ_r^3 :

$$\frac{\rho}{\sigma_D^\epsilon} \propto r^{-\alpha}, \quad (5)$$

where $\sigma_D = \sigma_r \sqrt{1 + D\beta}$, and D parameterizes a generalized σ_D ; for instance, $D = 0, -2/3$ and -1 correspond to $\sigma_D = \sigma_r, \sigma_{\text{tot}}$ (1-d), and σ_t , respectively. Schmidt et al. (2008) showed that the best-fit values of (D, ϵ, α) differ from halo to halo, and as a set, they roughly follow the linear relations $\epsilon = 0.97D + 3.15$ and $\alpha = 0.19D + 1.94$. For $\sigma = \sigma_r$ (i.e. $D = 0$), the optimal relation is $\rho/\sigma_r^{3.15} \propto r^{-1.94}$, which is consistent with the reported behavior of ρ/σ_r^3 in N -body simulations within error bars. However, few haloes' best-fit value of D in Schmidt et al. (2008) is near $D = 0$.

To assess whether any of these relations is closer to a power-law than ρ/σ_r^3 in our calculations, we choose three sets of D and ϵ from their linear relation, $(D, \epsilon) = (0, 3.15), (-2/3, 2.50)$, and $(-1, 2.18)$, and plot in Fig. 3 the logarithmic slopes of these three relations ρ/σ_D^ϵ , using our solutions of the Jeans equation with non-zero β shown in Fig. 2. For clarity, only the three Einasto profiles are shown in Fig. 3, although our conclusions apply to the GNFW profiles as well. The three solid curves in Fig. 3 (for $D = 0$) represent $\rho/\sigma_r^{3.15}$, and are therefore very similar to the short-dashed curves for the Einasto ρ/σ_r^3 in Fig. 2. The other two

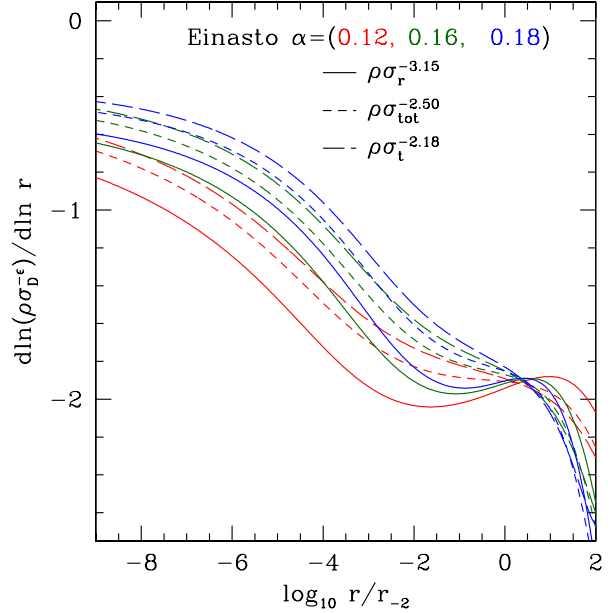


Figure 3. Radial dependence of three examples of the general density-velocity relation ρ/σ_D^ϵ (Schmidt et al. 2008) obtained from our calculations: $\rho/\sigma_r^{3.15}$ (solid), $\rho/\sigma_{\text{tot}}^{2.5}$ (short-dashed), and $\rho/\sigma_t^{2.18}$ (long-dashed). The y -axis shows the logarithmic slopes of these relations. The input β is from equation (4), and the input ρ are the three Einasto profiles shown in Figs. 1 and 2. This figure illustrates that like ρ/σ_r^3 , ρ/σ_D^ϵ is also far from being a power-law over the wide range of radius shown.

sets of curves in Fig. 3 suggest that $\rho/\sigma_{\text{tot}}^{2.5}$ (i.e. $D = -2/3$) and $\rho/\sigma_t^{2.18}$ (i.e. $D = -1$) are also far from being a power-law over the wide range of radius shown. When it is limited to the range of $0.01 \lesssim r/r_{-2} \lesssim 10$ probed by simulations, $\rho/\sigma_{\text{tot}}^{2.5}$ appears to be slightly closer to a power-law than ρ/σ_r^3 for the $\alpha = 0.12$ (red) and 0.16 (green) Einasto profiles. Over the larger range of radius shown in Fig. 3, however, our earlier conclusion of a non-power-law ρ/σ_r^3 carries over to the broader range of ρ/σ_D^ϵ shown.

4 FORCING ρ/σ_r^3 TO BE A POWER LAW

Thus far we have solved the Jeans equation assuming an input $\rho(r)$. As a point of comparison, we have also solved the Jeans equation following the works of previous authors with a starting assumption of a power law $\rho/\sigma_r^3 \propto r^{-\eta}$. Most notably, Taylor & Navarro (2001) presented results for the special case of $\eta = 15/8 = 1.875$, whereas Dehnen & McLaughlin (2005) (see also Austin et al. 2005) argued that only a single *realistic* solution exists for ρ , given when η takes the particular value of $35/18 = 1.9444$ for isotropic velocities, and $\eta = 35/18 - 2\beta_0/9$ for anisotropic velocities, where $\beta_0 \equiv \beta(r = 0)$.

Here we examine a range of η and show in Fig. 4 our numerical solutions (for $\beta = 0$) from the Jeans equation for $\rho(r)$ for four values of input power-law $\rho/\sigma_r^3 \propto r^{-\eta}$: $\eta = 1.8, 1.875, 1.9444$ and 2.0 . As η moves away from the critical value 1.9444 , ρ drops to zero rapidly at some small radius if $\eta > 1.9444$ (short-dashed curve), while ρ is cut-

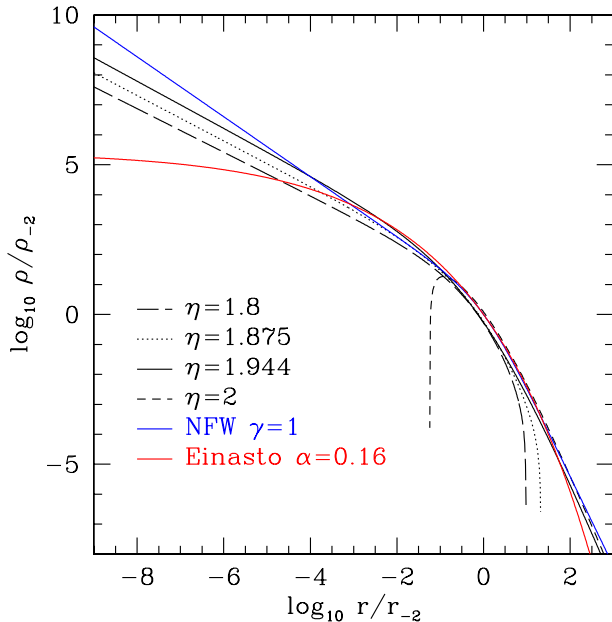


Figure 4. Solutions for $\rho(r)$ computed from the spherical Jeans equation with an input power-law $\rho/\sigma_r^3 \propto r^{-\eta}$ and $\beta = 0$. Four values of η are shown. Only when η is in the range between ~ 1.8 and 1.9444 does the solution not contain unphysical holes at small r (e.g. $\eta = 2$) or excessive cutoffs at large r . The shapes of ρ in this narrow range of η , however, deviate significantly from both the Einasto (solid red) and $\gamma = 1$ GFW (solid blue) profiles at small radius. Dark matter haloes therefore cannot follow the Einasto ρ and a power-law ρ/σ_r^3 simultaneously at all radii.

off sharply at some large r if $\eta < 1.9444$ (long-dashed and dotted curves). The former solution with a central hole is unphysical for dark matter haloes. The latter, however, is not automatically ruled out. Only for $\eta \lesssim 1.8$ do we find the outer ρ to drop off too steeply to represent realistic Λ CDM haloes. It therefore appears that the narrow range of $1.8 \lesssim \eta \leq 1.9444$ may admit physical solutions for ρ . It is important to keep in mind, however, that ρ in these cases are not well described at small radius by either the Einasto profile advocated by recent simulations, or the original $\gamma = 1$ GFW profile. Lowering the inner slope of the GFW profile to $\gamma \approx 0.75$ provides a better fit. Dark matter haloes therefore cannot be well fit by the Einasto ρ and a power-law ρ/σ_r^3 simultaneously at all radii.

5 CONCLUSIONS

Motivated by the apparent power-law radial profile of the pseudo-phase space density, ρ/σ_r^3 , reported in various N -body simulations (e.g., Taylor & Navarro 2001; Ascasibar et al. 2004; Dehnen & McLaughlin 2005; Hoffman et al. 2007; Stadel et al. 2008; Navarro et al. 2008), we solve the Jeans equation to study the *implied* pseudo-phase-space density for given parameterizations of ρ suggested by N -body simulations, i.e., Einasto and GFW. We find that independent of the velocity anisotropy, ρ/σ_r^3 is not a pure power law in radius for either the Einasto or GFW profiles (left panels of Fig. 1). In the radial ranges that are probed by current

N -body simulations (down to $\sim 10^{-3}r_{vir} \sim 10^{-2}r_{-2}$), we find that ρ/σ_r^3 happens to be approximately a power law, in particular for the Einasto profile (right panels of Fig. 1). For radial scales right below the resolution of current simulations, however, we see significant deviations from a power law profile for ρ/σ_r^3 if either Einasto or GFW continues to hold as a suitable parameterization of ρ . This result is unchanged when velocity anisotropy is included in the calculation (Fig. 2), and when a more general density-velocity relation of ρ/σ_D^6 is considered (Fig. 3). The hope to gain deep insight into the process of dark matter halo formation using a simple and universal power law scaling of ρ/σ_r^3 may therefore be misleading. Conversely, when $\rho/\sigma_r^3 \propto r^{-\eta}$ is assumed as an input in the Jeans equation, none of the realistic solutions for ρ , which occur only for the narrow range of $1.8 \lesssim \eta \leq 1.9444$, take the Einasto form (Fig. 4).

We therefore conclude that the two halo properties seen in current simulations – the Einasto ρ and power-law ρ/σ_r^3 – cannot hold simultaneously at all radii. We expect that the upcoming simulations with better spatial resolution will settle this debate: either the Einasto profile will continue to hold and ρ/σ_r^3 will show a break from a power law, or ρ/σ_r^3 will continue as a power law inward and ρ will deviate from its current parameterizations.

We thank Onsi Fakhouri, Peng Oh, and Simon White for useful discussions. PC and JZ are supported by the Theoretical Astrophysics Center at UC Berkeley.

REFERENCES

- Ascasibar Y., Yepes G., Gottlöber S., Müller V., 2004, MNRAS, 352, 1109
- Austin C. G., Williams L. L. R., Barnes E. I., Babul A., Dalcanton J. J., 2005, ApJ, 634, 756
- Dehnen W., McLaughlin D. E., 2005, MNRAS, 363, 1057
- Dubinski J., Carlberg R. G., 1991, ApJ, 378, 496
- Einasto J., 1969, Astrofizika, 5, 137
- Graham A. W., Merritt D., Moore B., Diemand J., Terzić B., 2006, AJ, 132, 2701
- Hansen S. H., 2004, MNRAS, 352, L41
- Hansen S. H., Moore B., 2006, New Astronomy, 11, 333
- Hernquist L., 1990, ApJ, 356, 359
- Hoffman Y., Romano-Díaz E., Shlosman I., Heller C., 2007, ApJ, 671, 1108
- Merritt D., Graham A. W., Moore B., Diemand J., Terzić B., 2006, AJ, 132, 2685
- Merritt D., Navarro J. F., Ludlow A., Jenkins A., 2005, ApJL, 624, L85
- Moore B., Quinn T., Governato F., Stadel J., Lake G., 1999, MNRAS, 310, 1147
- Navarro J. F., Frenk C. S., White S. D. M., 1997, ApJ, 490, 493
- Navarro J. F., Hayashi E., Power C., Jenkins A. R., Frenk C. S., White S. D. M., Springel V., Stadel J., Quinn T. R., 2004, MNRAS, 349, 1039
- Navarro J. F., Ludlow A., Springel V., Wang J., Vogelsberger M., White S. D. M., Jenkins A., Frenk C. S., Helmi A., 2008, ArXiv e-prints
- Press W. H., Teukolsky S. A., Vetterling W. T., Flannery B. P., 1992, Numerical Recipes. Cambridge Univ. Press, Cambridge

- Prugniel P., Simien F., 1997, *A&A*, 321, 111
Schmidt K. B., Hansen S. H., Macciò A. V., 2008, *ApJL*,
689, L33
Sersic J. L., 1968, *Atlas de galaxias australes*
Stadel J., Potter D., Moore B., Diemand J., Madau P.,
Zemp M., Kuhlen M., Quilis V., 2008, *ArXiv e-prints*
Taylor J. E., Navarro J. F., 2001, *ApJ*, 563, 483
Zait A., Hoffman Y., Shlosman I., 2008, *ApJ*, 682, 835